Caterina Capponi, Marco Ferrante, Aaron C. Zecchin, Jinzhe Gong

Leak detection in a branched system by inverse transient analysis with the admittance matrix method

Water Resources Management, 2017; 31(13):4075-4089

Noname manuscript No.
(will be inserted by the editor)

Leak detection in a branched system by inverse transient analysis with the admittance matrix method

Caterina Capponi · Marco Ferrante · Aaron C. Zecchin · Jinzhe Gong

Received: date / Accepted: date

Abstract The diagnosis of water distribution systems by means of the inverse transient analysis requires efficient and reliable numerical models. In the network admittance matrix method (NAMM) the 1-D waterhammer governing equations are integrated in the frequency domain and organized in a laplacian matrix form. The NAMM is particularly suitable for complex systems because of this structure and can be used for the system diagnosis, including leak sizing and location. In this paper a damaged branched system is considered and the diagnosis is performed by means of the NAMM using experimental data from laboratory transient tests. Two different boundary conditions are used in the implementation of the NAMM and the leak is located and sized with a reasonable approximation. An extended numerical investigation is also presented and allows confirmation of the results for different leak locations. The use of the NAMM for the leak detection and the validation using experimental data on a branched system are the main original contributions of this work. The successful diagnosis indicates promising results for applications in more complex systems.

Keywords Branched system · Diagnosis · Frequency domain · Leak · Transients · Water distribution systems

C. Capponi
via G. Duranti 93, 06125, Perugia, Italy
Tel.: +39-075-5853893
Fax: +39-075-5853892
E-mail: caterina.capponi@studenti.unipg.it

1 Introduction

Inverse transient analysis (ITA) is a technique for the diagnosis of pressurized pipe systems, based on the use of transients (Liggett and Chen, 1994). With respect to other techniques, transients are a cheap and fast tool to collect information about the system under consideration (Covas and Ramos, 2010; Kapelan, Savic, and Walters, 2003; Pezzinga, Brunone, and Meniconi, 2016; Shamloo and Haghighi, 2010; Soares, Covas, and Reis, 2011; Stephens, Lambert, and Simpson, 2012; Tuck and Lee, 2013; Vitkovsky, Lambert, Simpson, and Liggett, 2007; Vitkovsky, Lambert, Simpson, Wang, et al., 2001).

The ITA implementation can be highly iterative, requiring many simulations of the numerical model. Consequently, the choice of the numerical model plays a crucial role in terms of computational efficiency (Creaco and Pezzinga, 2015).

In the case of complex systems, frequency-domain models present an interesting trade off between accuracy and speed. With respect to time-domain models, they do not need a time-space grid with constant steps for the integration of the transient governing equations and as a consequence they allow a relatively fast and efficient modeling. The linearization errors related to the steady-friction can be checked and are often negligible, when compared to viscoelasticity or unsteady-friction, which, in addition, are easy to implement in these models (Kim, 2005; Weinerowska-Bords, 2006).

The network admittance matrix method (NAMM) proposed by Zecchin, Simpson, Lambert, White, and Vitkovsky (2009) is a frequency-domain model that organizes the transient governing equations for each link of a network in a laplacian matrix form. Its elegant structure makes this model appealing for the analysis of the response of complex systems to transients and for their diagnosis (Zecchin, Lambert, Simpson, and White, 2014).

Frequency-domain models have been used for leak detection in the case of simple systems (e.g., Gong, Lambert, Simpson, and Zecchin, 2013; Gong, Lambert, Zecchin, and Simpson, 2015; Gong, Zecchin, Simpson, and Lambert, 2014; Lee, Vítkovský, and Lambert, 2005a; Lee, Vítkovský, Lambert, Simpson, and Liggett, 2005b; Lee, Vítkovský, Lambert, Simpson, Liggett, and Murray, 2004; Sun, Wang, and Duan, 2016), also with the implementation of viscoelasticity (Duan, Lee, Ghidaoui, and Tung, 2012). With reference to the modeling of more complex systems there are few studies in the time domain (Evangelista, Leopardi, Pignatelli, and de Marinis, 2015; Ferrante, Brunone, and Meniconi, 2009), while in the frequency domain (Kim, 2008), only a few papers explore the leak detection by means of numerical signals (Duan, 2017; Duan, Lee, Ghidaoui, and Tung, 2011; Kim, 2015), with none, to the authors knowledge, using experimental data.

In this paper a frequency domain model based on NAMM is used for the leak detection by means of ITA in an experimental branched system. The pressure dependent demands at nodes are implemented in the model to simulate the leak occurrence and the effects of the maneuver giving raise to the transient are simulated either with a flow or pressure variation at the valve node. These two different boundary conditions for the maneuver node give place to two models that can be used for the analysis. The results for both cases are presented in this paper, together with some interesting remarks.The structure of the NAMM allows an easy implementation of one or more leaks and the choice of the leak location and size as parameters for calibrations. It is worth noting that the NAMM, until now, has not been used yet for leak detection purposes. The calibration procedure for leak detection and sizing for the considered system is based on a NAMM model and on two optimization algorithms, in series: a genetic algorithm (Creaco and Pezzinga, 2015; Pezzinga et al., 2016; Vitkovsky, Simpson, and Lambert, 2000) and a nonlinear optimization algorithm (Lagarias, Reeds, Wright, and Wright, 1998). Such a calibration procedure is tested on experimental data acquired on a branched system with a leak, at the Water Engineering Laboratory (WEL) of the Department of Civil and Environmental Engineering at the University of Perugia, Italy. The detection is performed considering the branch where the leak is as known or unknown. This different starting hypothesis allows a generalization of the calibration results for more realistic situations. To explore the robustness of the ITA, different leak locations are also considered in a numerical investigation, where simulated pressure signals are used instead of measured data.

The use of the NAMM for the leak detection and the validation using experimental data on a branched system are the main original contributions of this work. The calibration procedure for leak detection in the case of unknown branch is one of the novelties of the paper. The results presented in this work represent an important step forward the diagnosis of water distribution systems.

2 Forward modeling using the admittance matrix model with a leak

In frequency-domain modeling, the 1-D waterhammer governing equations are firstly perturbed and linearized, and then integrated in the frequency domain (Chaudhry, 2014). In the model based on the network admittance matrix method (NAMM) these equations are reorganized in a laplacian matrix form, as shown by Zecchin et al. (2009). The obtained formulation entails only nodal variables. In fact, this formulation relates the vector of the transformed nodal flows, $\mathbf{\Theta}(\omega)$ (where a positive flow is considered as a flow into the network), to the vector of the transformed nodal pressures, $\mathbf{\Psi}(\omega)$, by means of the admittance matrix, $\mathbf{Y}(\omega)$

$$\mathbf{Y} \cdot \left[\Psi_1 \cdots \Psi_{\mathrm{k}} \cdots \Psi_{\mathrm{n}} \right]^T = \left[\Theta_1 \cdots \Theta_{\mathrm{k}} \cdots \Theta_{\mathrm{n}} \right]^T \tag{1}$$

with n the number of nodes in the system.

$\mathbf{Y}(\omega)$ contains the system dynamics and is defined with a compact notation as

$$\{\mathbf{Y}(\omega)\}_{i,k} = \begin{cases} -s_j, & \text{if nodes } i \text{ and } k \text{ are linked} \\ \sum_{\lambda_j \in \Lambda_i} t_j, & \text{if } k = i \\ 0 & \text{otherwise} \end{cases} \tag{2}$$

where λ_j is the $j-$th link of the system, Λ_i is the set of links incident to node i, ω is the angular frequency and

$$t_j(\omega) = [Z_{cj}(\omega)\tanh\Gamma_j(\omega)]^{-1} \;;\; s_j(\omega) = [Z_{cj}(\omega)\sinh\Gamma_j(\omega)]^{-1} \tag{3}$$

In Eqs. (3) $\Gamma_j = \gamma_j l_j$, with γ_j, l_j and Z_{cj} being the propagation operator, the length and the characteristic impedance for the $j-$th link, respectively (Wylie and Streeter, 1993). Eqs. (3) point out an interesting characteristic of the NAMM and of the other frequency domain based models, i.e. the implementation of the pipe lengths, l_j, as parameters. This feature is relevant for the leak location problem, as shown in the following.

To relate the unknown nodal pressure and flows to the known nodal conditions, two different types of nodes are distinguished: at the pressure controlled nodes, indicated by the subscript "p", the nodal pressure is known but the outflow is unknown, while at the demand nodes, indicated by the subscript "d", the nodal flow is known but the pressure is unknown. Junctions are typically demand nodes whereas reservoirs are pressure nodes.

Since the transformed nodal values of the pressures, Ψ, represent the perturbations around the mean values of the pressure head, a prescribed pressure head at a node, such as at a constant head reservoir, corresponds to $\Psi_p = 0$. Similarly, the transformed values of the flows, Θ, represent the variation of the negative of the demand at a node. Hence, when a junction without a demand is considered, it has $\Theta_d = 0$.

The occurrence of a leak, i.e. a pressure dependent demand, at the $k-$th node of a system is modeled in the frequency domain framework as

$$\Theta_k = -\frac{\Psi_k}{Z_{Lk}} \tag{4}$$

where the leak impedance, Z_{Lk}, depends on leak size and on the initial steady-state value of the pressure at the leak, as shown by Ferrante, Brunone, Meniconi, Karney, and Massari (2014). Hence, the leak takes effect on Eq. (2) introducing a term to the $k-$th element of the main diagonal of $\mathbf{Y}$, which becomes $\mathbf{Y} + \text{diag}\left\{0, \cdots, \frac{1}{Z_{Lk}}, \cdots, 0\right\}$. The incorporation of leaks and other nodal dynamic elements into the NAMM is considered in detail in Zecchin, Lambert, and Simpson (2010).

The distinction between the conditions of demand control and pressure control nodes allows the uncoupling of the unknowns from the known variables. The transformed nodal pressures at each node of the system can be determined once the corresponding partitions of $\mathbf{Y}$ are inverted. The pressure and flow signals in the time domain, $H(t)$ and $Q(t)$, respectively, can then be evaluated by means of the inverse Fourier transform.

Given the distinction between pressure and demand nodes, the effects of the maneuver can be simulated in terms of a pressure or demand variation, giving place to two different models. In the following both models are considered. Model 1 uses a demand control condition at the maneuver node, which means that the flow signal is introduced as the input and the pressure is calculated as an output at the demand node. On the contrary, Model 2 uses a pressure control condition at the maneuver node, which means that the acquired pressure signal is used as the input at a pressure node and the flow is calculated as an output.

3 Leak detection in pipe networks by means of the admittance matrix method

In the ITA, the model parameters are calibrated, i.e. they are varied in a set of simulations to reproduce, as close as possible, the measured pressure signals.

In this research, the objective function used for the calibration to measure the distance between simulated and observed data is

$$\sigma^2 = \frac{\sum_{i=1}^{n}(O_i - P_i)^2}{n} \tag{5}$$

where O_i, P_i, are two sets of measured and simulated data of length n, respectively.

Two algorithms in series are used to minimize σ^2 and solve the inverse problem: a genetic algorithm, also referred to as GA, and an unconstrained nonlinear optimization algorithm, referred to as NOA, based on the Nelder-Mead algorithm. The GA is used as a first step to explore a wide area and provide a rough estimate of the local minimum. NOA is used as a second step starting from the GA solution to provide a more accurate estimate.

4 Experimental verification

An experimental branched system is considered and used to assess the utility of the calibration procedure in determining the leak location and size. The

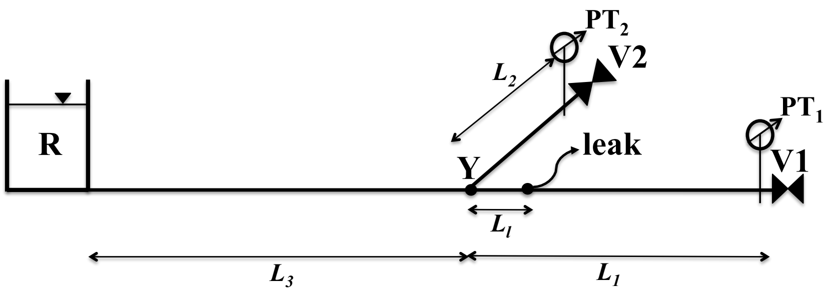

Fig. 1 Schematic of the damaged branched system installed at the Water Engineering Laboratory (WEL) of the Department of Civil and Environmental Engineering (DICA) at the University of Perugia, Italy.

leak is located on one branch and the procedure is tested by considering both the cases of (1) knowing the branch on which the leak is located (but the leak location on the branch and size are unknown), and (2) not knowing the branch on which the leak is located (again, the location and size are also unknown). To extend the investigation to the cases of a single leak in one of the other two branches, the signals produced by numerical models are used instead of the acquired signals.

4.1 Experimental setup and measured data

The branched system of Fig. 1, hereafter referred to as the Y-system, was installed at the Water Engineering Laboratory (WEL) of the Department of Civil and Environmental Engineering at the University of Perugia, Italy. It consisted of 3 HDPE pipes of lengths $L_1 = 116.78$ m, $L_2 = 61.78$ m and $L_3 = 197.82$ m, with internal diameter $D = 93.3$ mm and wall thickness $e = 8.1$ mm. The pipes were bounded via a reservoir (R), a junction (Y) and two valves (V1 and V2). Valve V1 was kept closed (i.e., it was a dead end) while V2 was the operating valve used to induce the transient into the system. Two pressure transducers, PT_1 and PT_2, were placed immediately upstream of V1 and V2, respectively. The signals were measured at a sampling frequency, f, of

1000 Hz and downsampled to 100 Hz to decrease the noise level and to speed up the assessment of the calibration procedure. The downsampling frequency of 100 Hz was selected, as at this sampling frequency much of the features of the transient signal were retained. The initial steady-state flow at V2, q_0, was 3.0 l/s, with an uncertainty of 0.25%. Along the branch between the Y junction and the dead end node, a leak was placed at a distance $L_l = 24.18$ m from the Y junction. The leak was simulated by means of a device with a circular hole of 14.9 mm diameter and was characterized by an effective area $\mu\Sigma = 1.101\ 10^{-4}$ m^2 and a relative size $\mu\Sigma/A = 0.0162$, with A being the pipe cross-sectional area (Ferrante et al., 2014). Considering that the value of the piezometric head at the leak in steady-state conditions was measured as $\bar{H}_L = 21.3$ m, the outflow at the leak was $\bar{Q}_L = 2.3$ l/s and the leak impedance was $Z_L = 2\bar{H}_L/\bar{Q}_L = 1.8522\ 10^4$ s/m^2. The steady-state flow ratio was $\bar{Q}_L/(q_0 + \bar{Q}_L) = 0.434$ and the impedance ratio (Ferrante et al., 2014) was $Z_L/Z_c = Z_L gA/a = 3.283$, with g being the gravitational acceleration. The wave speed a=378.18 m/s was determined by a calibration process based on the tests on the same experimental system without the leak. The procedure is described in Ferrante and Capponi (accepted). The pressure signals acquired by PT_2 and PT_1 are shown in time in Fig. 2a and 2b, respectively. The rheological properties of the pipe material had been previously investigated on the intact system and are considered as known for the purposes of this investigation. Three Kelving-Voigt (KV) elements in series are used, with viscosity coefficients $\eta_{R-1,2,3} = 8.35\ 10^7$, $5.82\ 10^9$, $2.96\ 10^9$ Pa s, respectively, and relaxation moduli $E_{R-1,2,3} = 1.88\ 10^{10}$, $1.98\ 10^{10}$, $4.24\ 10^{10}$ Pa, respectively.

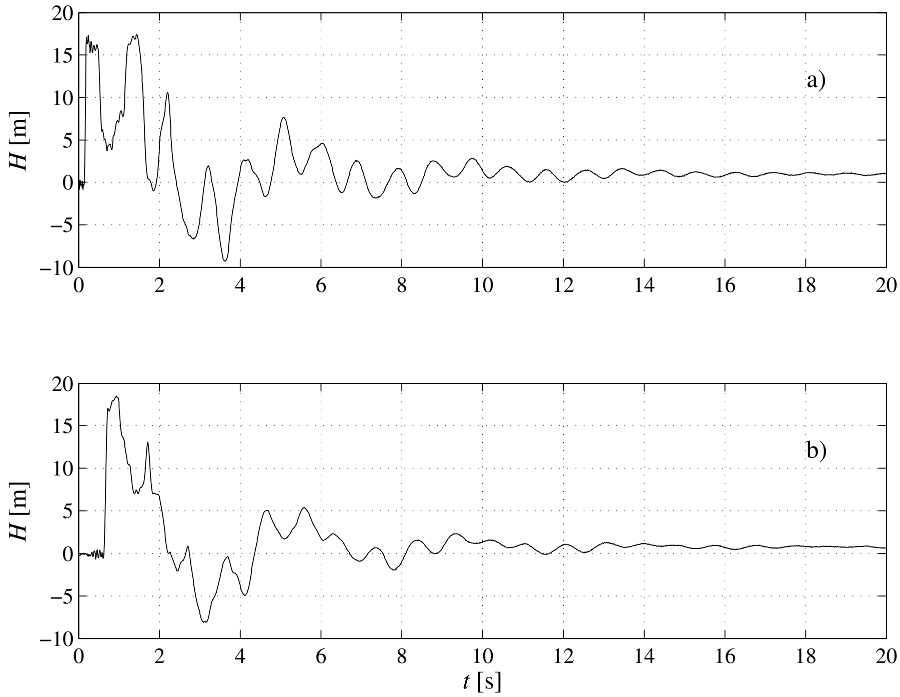

Fig. 2 Pressure signals measured at PT_2 (a) and PT_1 (b), respectively.

4.2 Inverse calibration and results

The two unknowns in the system of Fig. 1, i.e. the location and the size of the leak, are estimated by means of the two step calibration procedure involving a GA and a NOA in series. As mentioned above, the location is expressed by the distance of the leak from the Y junction, L_l, while the size is expressed in terms of leak impedance, Z_L. The GA and the NOA minimize the differences between the measured pressure signal and the pressure signal simulated by means of the NAMM.

The availability of pressure signals at two different locations allows the use of both Model 1 and Model 2. The calibration based on Model 1 uses the transient flow signal simulated at the maneuver node. For these purposes, the pressure signal during the maneuver duration is used to estimate the variation of the flow at V2 (Brunone and Morelli, 1999). The flow variation is then

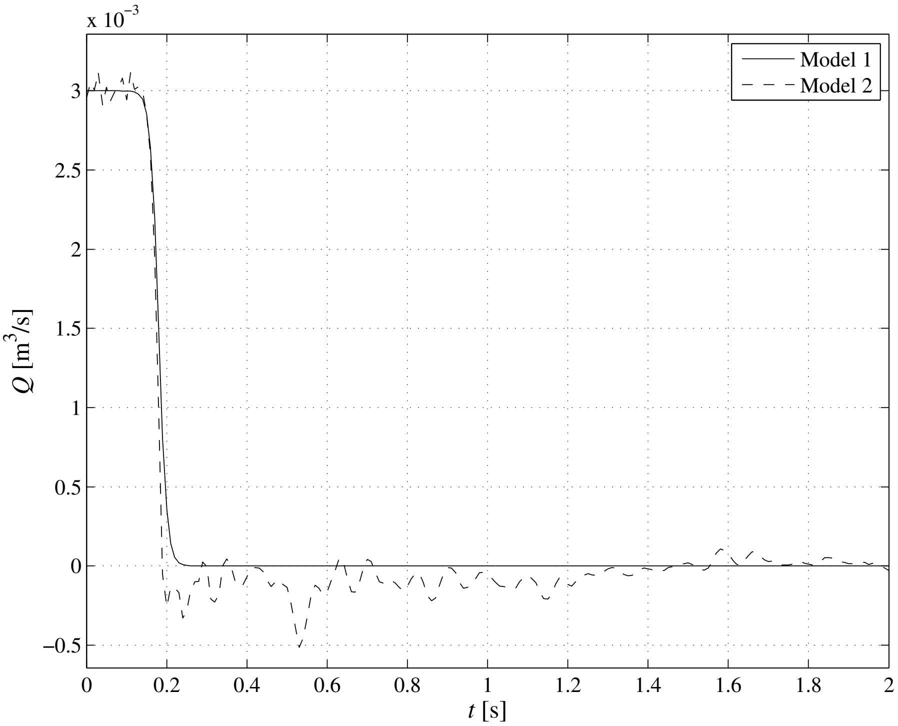

Fig. 3 Comparison in time domain between the flow modeled as a complete and fast closure in the case of Model 1 (solid line) and the flow obtained by Model 2 (dashed line) using the acquired pressure signal at immediately upstream V2 as the input.

considered as known at the valve demand node (Fig. 3) and the numerical pressure signals are simulated at the measurement sections, PT_1 and PT_2. The calibration is based on the comparison of the observed and simulated pressure signal at PT_2, while the observed and simulated signals at measurement section PT_1 are only compared for validation.

Model 2 directly uses the pressure signal as an input at the valve node, considered as a pressure controlled node. As a consequence, in this case the calibration is made by means of the comparison of experimental and numerical signal only at the PT_1 section, and no validation is undertaken.

Table 1 Results of the calibrations of the leak location and size by means of Model 1 and Model 2, using a GA and a NOA in series. The errors are referred to the experimental values of L_l (absolute error) and Z_L (relative error).

Calibration by	σ^2_{min} [m^2]	Results		Absolute Error	Relative Error
		L_l [m]	Z_L [s/m^2]	in L_l [m]	in Z_L [%]
Model 1	0.1110 (M1)	24.7349	1.5887 10^4	0.5549	14.23
	0.0255 (M2)				
Model 2	0.0250	23.2121	1.5891 10^4	0.9679	14.20

4.2.1 Leak location and sizing on a known branch

As a first step, the branch where the leak is placed is assumed to be known and the leak location is estimated. As previously mentioned, instead of the time-domain models, which point out the nodes closest to the leak, the chosen frequency-domain model allows the calibration of an unknown length as a parameter.

The bounds for the parameter L_l are set equal to zero for the lower bound and to L_1 for the upper bound. Regarding the size, the bounds for the leak impedance are assumed as $[5\,10^3; 3\,10^5]$ s/m^2. For each GA run a maximum number of 50 generations is set with a population size of 100 individuals. The starting point for the GA is set to the middle of the range defined by the mentioned bounds. The GA solution is then used as the starting point for the NOA. The NOA results obtained by means of Model 1 and Model 2 are summarized in Table 1, where the errors with respect to the experimental values of the two calibrated parameters are also reported.

The values of σ^2 in the second column are evaluated by Model 1 both at PT_1, as minimized by the calibration procedure, and PT_2, only for validation purposes. The value of σ^2 for Model 2 is minimized considering the signals at PT_2 since the signal at PT_1 is used as input.

Based on the comparisons of the results (Fig. 4), it seems that Model 2 has the important advantage that it captures the deterministic components of the signal at the valve that is not properly described by the estimated maneuver characteristics and it can reproduce the small oscillation of the signal, that are not due to the noise, better than Model 1.

The leak location and size obtained by the calibration using Model 1 are used to simulate the transient at the maneuver node with Model 1 and at the dead end node with Model 2. These signals, denoted by “M1” and “M2”, respectively, are compared in Fig. 4 with the observed pressure signals, denoted by “exp”. Fig. 4a shows the comparison of the experimental signal at the dead end node with the numerical one simulated by means of Model 2 using the values of leak location and size calibrated by means of Model 1. The same values are used in Model 1 to generate the signal at the maneuver node shown in Fig. 4c. In Fig. 4b (Fig. 4d) the comparison of Fig. 4a (Fig. 4c) is shown for the time, t, ranging from 0 to 4 s.

When the leak location and size are calibrated by means of Model 2, the experimental signal at the maneuver node is used as the input so it cannot be exploited for comparisons and for the evaluation of σ^2. Therefore, in this case, only the signal acquired at the dead end node is used for the minimization of σ^2 and the result is shown in Tab. 1. The minimum value of σ^2 is very similar to the one obtained with the same model in the calibration based on Model 1. Moreover, the relative error in the leak sizing is similar for the two models, but the absolute error in the location is slightly higher in Model 2 than in Model 1. The comparison between the experimental signal and the signal simulated by Model 2 using these results is shown in Fig. 5. Also, at a closer look (Fig. 5b) it can be observed that, as in the previous calibration, the signals are almost indistinguishable. To give an insight into the calibration, the shape of the objective function over the entire parameter space is shown

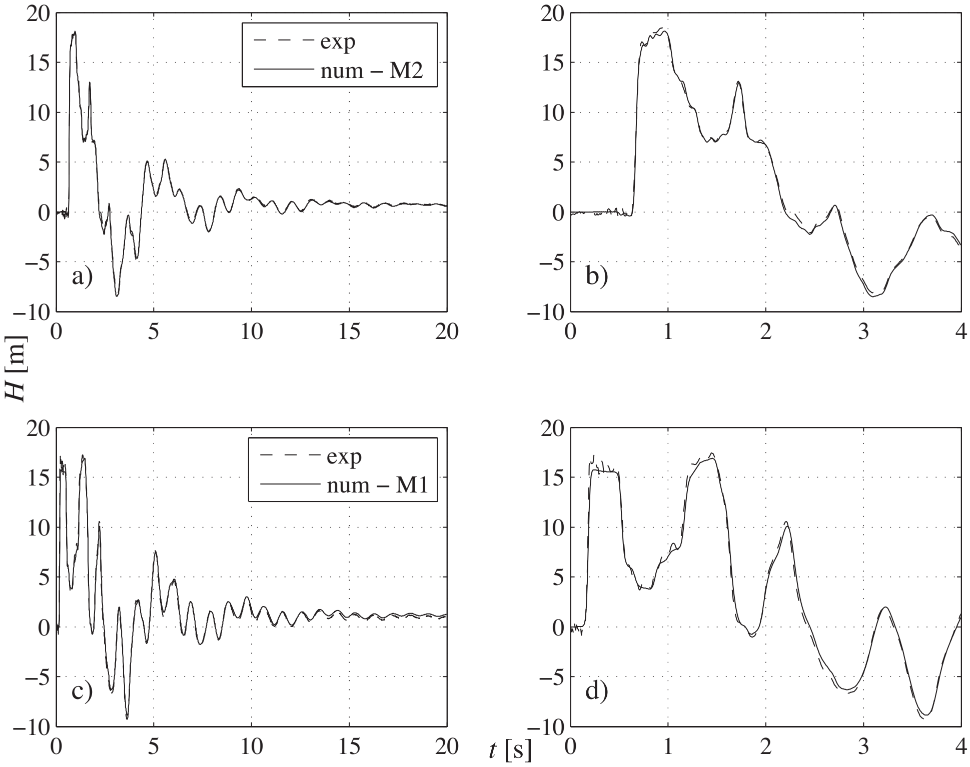

Fig. 4 Comparison of the experimental signals at the dead end node (a) and at the maneuver node (c) with the signals simulated by Model 2, M2 (a), and by Model 1, M1 (c), using the leak location and size calibrated by means of Model 1 at the maneuver node. In (b) and (d) the same comparisons of (a) and (c) are shown for t ranging from 0 to 4 s, respectively.

in Fig. 6. The existence of two calibrated parameters allows its visualization on a surface plot. The range of variation of the leak location and size are split in 100 parts giving place to a grid of 10^4 points. At each point σ^2 is evaluated comparing the experimental signal with those simulated by means of Models 1 at the maneuver node. The white cross indicates the values of the location and the size found by the optimization algorithm and shown in Tab. 1.

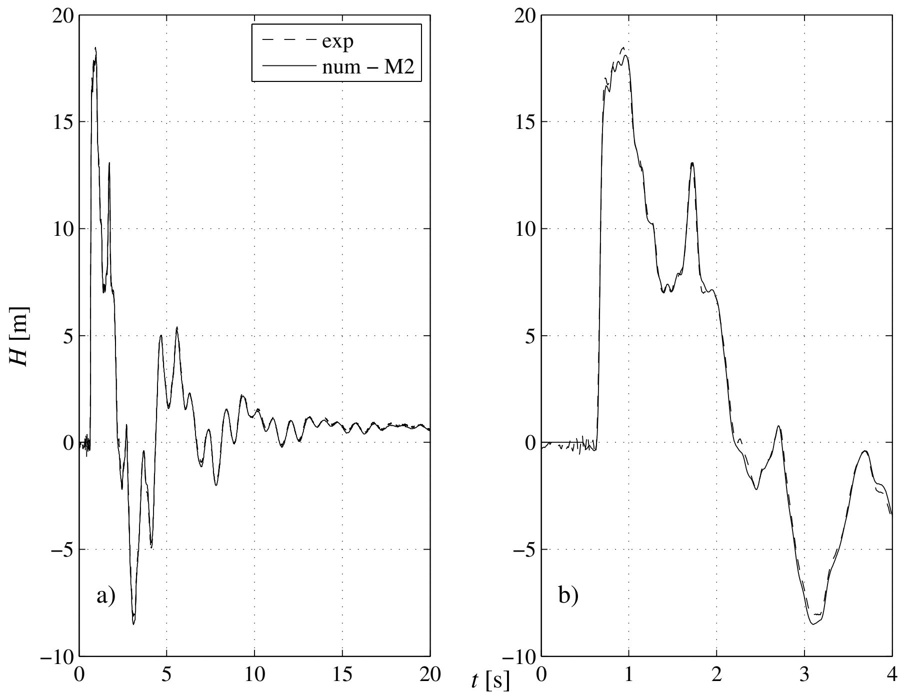

Fig. 5 Comparison of the experimental signal at the dead end node with the signal simulated by Model 2, M2, using the leak location and size calibrated by means of Model 2. In (b) the same comparisons of (a) is shown for t ranging from 0 to 4 s.

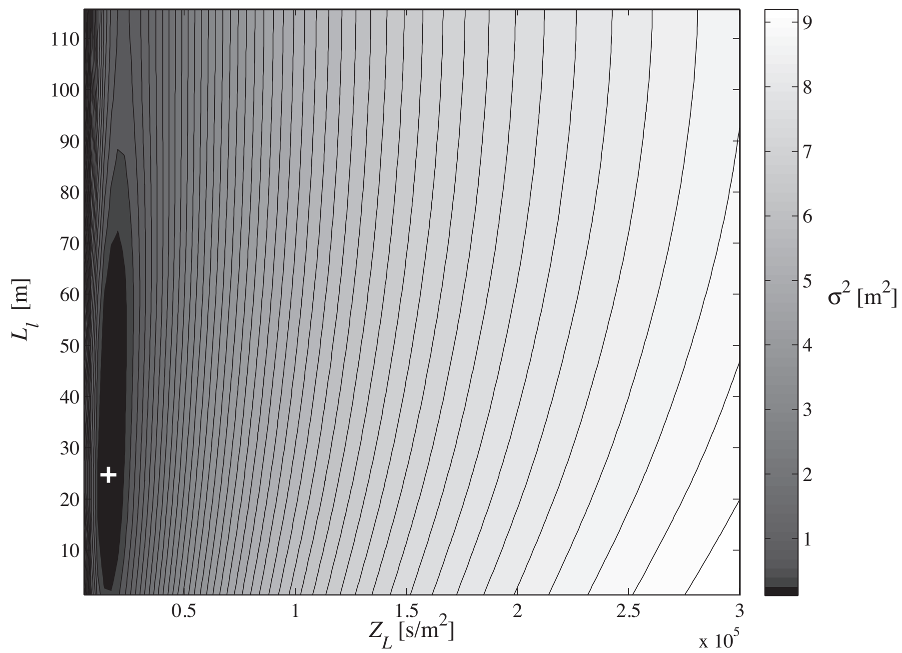

Fig. 6 Surface plot of the variation of σ^2 with L_l and Z_L evaluated by means of Model 1. The white cross indicates the values of L_l and Z_L found by the GA and the NOA and shown in Tab. 1.

4.2.2 Unknown branch

The calibration results shown so far are based on the assumption that the branch on which the leak is located is known. This assumption is optimistic but in the diagnosis of water pipeline systems it can happen that the branch containing the leak is unknown. For this reason a further calibration approach is carried out removing this assumption. The numerical model is set placing a leak node on each branch and performing a calibration by means of Model 1 that minimizes σ^2 in the comparison of experimental and numerical signal at the maneuver node. In this way there are 6 calibration parameters, i.e. 3 leak locations, expressed as distances from the Y junction, and 3 leak impedances, that indicate the sizes. The calibration based on the NAMM can be considered

Table 2 Results of the calibrations of the leak location and size by means of Model 1 and Model 2, using a GA and a NOA in series, in the case of unknown branch. The errors are referred to the experimental values of L_l (absolute error) and Z_L (relative error).

Calibration by	σ^2_{min} [m^2]	Results		Absolute Error	Relative Error
		L_l [m]	Z_L [s/m^2]	in L_l [m]	in Z_L [%]
Model 1	0.1110 (M1) 0.0255 (M2)	24.7349	1.5887 10^4	0.5549	14.23
Model 2	0.0218	24.3852	1.5740 10^4	0.2052	15.02

as successful if in the results the actual leak location and the corresponding leak size are as close as possible to the experimental ones and if the other 2 sizes (corresponding to leaks on the pipes that actually contain no leaks) are as small as possible (which correspond to leak impedances values as high as possible). The 2 locations that are estimated on the pipes that contain no leaks are not significant for the success of the calibration. The parameter bounds are set constraining the locations to the total lengths of the branches and allowing the leak impedances to vary up to 10^{20} s/m^2, which corresponds to a negligible leakage. The population size is set to 100 individuals and the maximum number of generations is 50, as in the previous cases. The GA solution does not suggest the most likely branch containing the leak and it is used as the starting point for the next step, the NOA. In a computational time of about 5512 s on an Intel Xeon 2.20 GHz computer, the NOA finds the same solution of the first calibration presented in this work: the minimum value of σ^2 is 0.1110 m^2, the leak impedance is $1.5887\,10^4$ s/m^2, and the leak location found is 24.7349 m from the Y junction along the branch connected to the dead end, as shown in Tab.2.

Besides the fact that the calibration procedure finds the same result as the previous case, when only one branch was used as candidate, the values found for the other parameters are interesting as well. The leak impedance values found for the leak nodes placed on the other branches are $5.0800\,10^{15}$

and $2.9499\,10^{15}$ s/m^2. This means that, regardless the locations found for these two leaks, they are estimated to be almost negligible in the size. In fact, the corresponding values of the effective area, $\mu\Sigma$, are $4.103\,10^{-16}$ and $7.066\,10^{-16}$ m^2, respectively. As a consequence, the numerical signal obtained by this calibration, carried out assuming the branch containing the leak as unknown, is practically the same as that of Fig. 4c,d.

The same procedure is followed using Model 2. The results are similar to those found in the previous case and are reported in Tab.2.

5 Extended numerical investigation

To investigate the reliability of the calibration procedure for different leak size and locations, a set of numerical tests has also been used, considering the same experimental setup used in the laboratory, but varying the leak location.

The leak considered within the numerical investigation is characterized by $\mu\Sigma = 3.36\ 10^{-5}$ m^2, $\bar{H}_L = 20$, and a relative size $\mu\Sigma/A = 0.0049$. The corresponding leak impedance is $Z_L = 6.0110\ 10^4$ s/m^2. The leak is placed on each branch, one at a time, at a distance of 20 m from the Y junction. Three numerical signals (Fig. 7) were generated at the valve V2 using these different locations and are considered as benchmarking in the calibrations, which are based on Model 1.

The same calibration procedure applied to the experimental data is used for the three numerical signals. For each branch the length parameter upper bound is set to the total length of the considered branch. The starting point is the middle of the range defined by the bounds.

In Tab. 3 the results of the numerical calibrations are reported. For each branch the solution that the calibration procedure has to find is indicated in the second column, while in the third one there is the total length, L_b, of

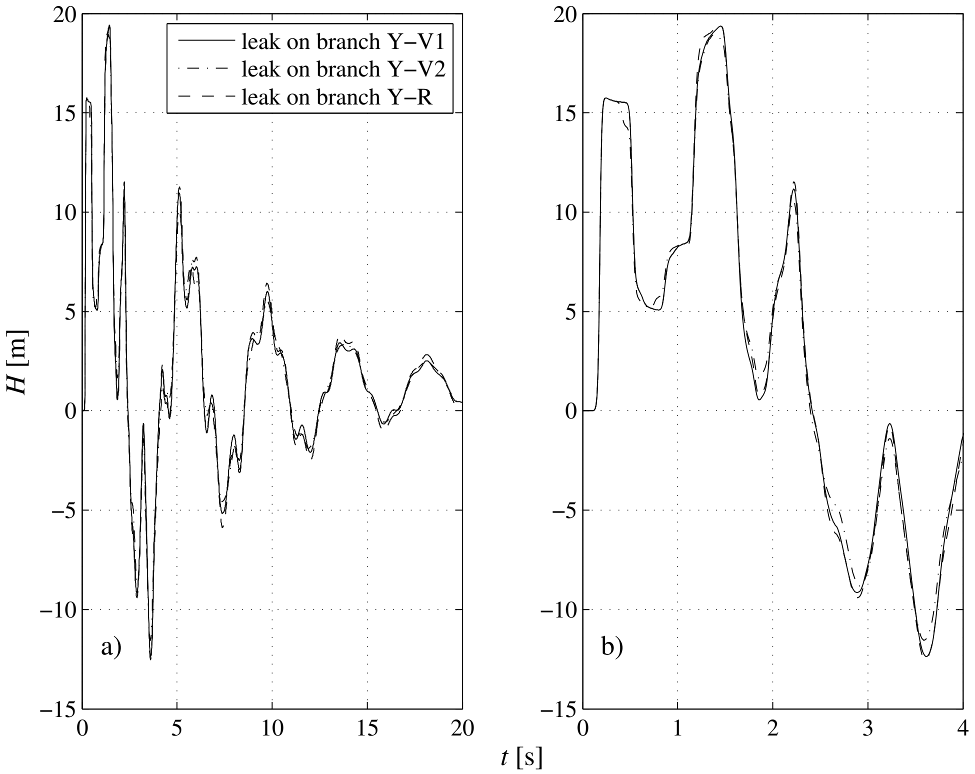

Fig. 7 Benchmark signals generated locating the leak on each branch of the system, one at a time. In (b) the same comparisons of (a) is shown for t ranging from 0 to 4 s.

each considered branch containing the leak. σ^2_{min} is the minimum value of the optimization function found by the GA and the NOA in series. Lastly, the "yes" in the last column indicates that all the numerical calibrations carried out have been successful in identifying the location of the leak.

These calibrations demonstrate that the procedure developed in this work is able to find a leak even smaller than that used in the experimental study and identify leaks in the other branches of the considered system.

Table 3 Results of the numerical calibrations of the leak location and size on the three branches.

branch with leak	L_l [m]; Z_L [s/m^2]	L_b [m]	σ^2_{min} [m^2]	identification
Y-V1		116.78	2.22 10^{-28}	yes
Y-V2	20; 6.0110 10^4	61.78	3.27 10^{-28}	yes
Y-R		197.82	1.39 10^{-28}	yes

6 Discussion

The admittance matrix method used for the calibration in this work is a key point in the diagnosis of the considered Y-system. It has the advantage of the ease in modeling complex systems and it requires a low computational effort with respect to time-domain models. Moreover, its structure allows the introduction of a link length (i.e., the leak location) as a calibration parameter, thus facilitating the diagnosis of the damaged system and avoiding the grid approximation problems typical of time-domain modeling, such as those due to a fixed time-space grid.

The chosen calibration procedure minimizes the optimization function, σ^2, in two steps, consisting of a GA and a NOA in series. The GA minimizes σ^2 starting from an initial value and exploring a wide range of the parameter space, but within certain bounds. The tests showed that, with the appropriate settings, the GA can be an efficient optimizer, but it was found to have some limits within our application, such as the fact that the individuals can gather around local minima instead of the global minimum. Furthermore, the global minimum location is found with a low accuracy. To reduce the risk of pointing out local minima, the conventional practice is to set a lot of populations with a large number of individuals. This increases the computational time, making the calibration procedure inefficient, with respect, for example, to the direct scrutiny of the optimization function on a regular grid. The NOA minimizes σ^2 starting from the GA solution and exploring a relatively narrow region around it, but without specified bounds. If the GA result is not too far from the solution, the NOA finds the global minimum with high accuracy and efficiency. The combination of these two steps allows the success of the diagnosis in all the cases considered in this work. When the experimental data are used, the diagnosis gives result close to reality, with a good approximation. On the other hand, when the numerical data are used, to assess the reliability of the procedure with a leak smaller than the leak size used in the experimental study, located also on the other branches, the minimum value of σ^2 has an order of magnitude of 10^{-28} m^2. Other issues that can affect the diagnosis results are the uncertainties in the system parameters and geometry, and those due to measurement noise. The noise for example can compromise the diagnosis because it can produce oscillations in the pressure signal that can be misinterpreted and lead to errors in the leak detection. Uncertainties in the system parameters and in the geometry can limit the utility of a model-based interpretation of the pressure signal and affect the calibration with significant error or even make it fail to correctly detect the leak. In the numerical investigation these uncertainties are not considered and this is the reason the values of σ^2 are so low (see Tab. 3). In the diagnosis of the system by means of the experimental data the uncertainties influence the results in the sense that σ^2 has higher, albeit reasonable (Tab. 1), values than in the numerical case-studies. Within the experimental study, the calibrated model was found to provide an excellent match to the observed pressure signal.

7 Conclusions

A frequency-domain model based on the network admittance matrix method (NAMM) is implemented in this paper and used within an inverse transient analysis on a branched system installed at the Water Engineering Laboratory

(WEL) of the Department of Civil and Environmental Engineering (DICA) at the university of Perugia, Italy. The ability to detect leaks on the considered system is tested both by experimental and numerical data and the detection is performed using two optimization algorithms in series. Regarding the experimental data, the detection is performed for different scenarios where the branch with the leak is considered as known or unknown, since the assumption that the branch where the leak is placed is known is optimistic and for this reason has been removed in the second step. In both cases, the leak is successfully detected, with an accuracy of less than 1 meter in the location and a relative error of about 14 % in the size. The numerical data are used to extend the investigation to the cases the leak is placed on the other branches and is characterized by a different size, smaller than the experimental one, with the aim to confirm the reliability of the detection procedure. In all the considered cases, the leak is successfully located and sized with high accuracy. Although the considered system is relatively simple and other time- and frequency-domain models could also be used, NAMM is particularly suited for complex systems and these results push towards the analysis of more complex systems.

Acknowledgements This research has been funded by the University of Perugia and by the Italian Ministry of Education, University and Research (MIUR) under the Project of Relevant National Interest "Tools and procedures for an advanced and sustainable management of water distribution systems".

References

Brunone, B., Morelli, L., 1999. Automatic control valve induced transients in an operative pipe system. Journal of Hydraulic Engineering, ASCE 125 (5), 534–542.

Chaudhry, M. H., 2014. Applied Hydraulic Transients. Springer.

Covas, D., Ramos, H., 2010. Case studies of leak detection and location in water pipe systems by inverse transient analysis. Journal of Water Resources Planning and Management-ASCE 136 (2), 248–257.

Creaco, E., Pezzinga, G., 2015. Embedding linear programming in multi objective genetic algorithms for reducing the size of the search space with application to leakage minimization in water distribution networks. Environmental Modelling & Software 69, 308–318.

Duan, H. F., 2017. Transient frequency response based leak detection in water supply pipeline systems with branched and looped junctions. Journal of Hydroinformatics 19 (1), 17–30.

Duan, H. F., Lee, P. J., Ghidaoui, M. S., Tung, Y. K., 2011. Leak detection in complex series pipelines by using the system frequency response method. Journal of Hydraulic Research 49 (2), 213–221.

Duan, H. F., Lee, P. J., Ghidaoui, M. S., Tung, Y. K., 2012. System Response Function–Based Leak Detection in Viscoelastic Pipelines. Journal of Hydraulic Engineering, ASCE 138 (2), 143–153.

Evangelista, S., Leopardi, A., Pignatelli, R., de Marinis, G., 2015. Hydraulic Transients in Viscoelastic Branched Pipelines. Journal of Hydraulic Engineering, ASCE 141 (8), 04015016–9.

Ferrante, M., Brunone, B., Meniconi, S., 2009. Leak detection in branched pipe systems coupling wavelet analysis and a Lagrangian model. Journal of Water Supply Research and Technology-Aqua 58 (2), 95–106.

Ferrante, M., Brunone, B., Meniconi, S., Karney, B. W., Massari, C., 2014. Leak Size, Detectability and Test Conditions in Pressurized Pipe Systems. Water Resources Management 28 (13), 4583–4598.

Ferrante, M., Capponi, C., accepted. Calibration of viscoelastic parameters by means of transients in a branched water pipeline system. Urban Water

Journal.

Gong, J., Lambert, M. F., Simpson, A. R., Zecchin, A. C., 2013. Single-Event Leak Detection in Pipeline Using First Three Resonant Responses. Journal of Hydraulic Engineering-Asce 139 (6), 645–655.

Gong, J., Lambert, M. F., Zecchin, A. C., Simpson, A. R., 2015. Experimental verification of pipeline frequency response extraction and leak detection using the inverse repeat signal. Journal of Hydraulic Research 54 (2), 210–219.

Gong, J., Zecchin, A. C., Simpson, A. R., Lambert, M. F., 2014. Frequency Response Diagram for Pipeline Leak Detection: Comparing the Odd and Even Harmonics. Journal of Water Resources Planning and Management 140 (1), 65–74.

Kapelan, Z. S., Savic, D. A., Walters, G. A., 2003. A hybrid inverse transient model for leakage detection and roughness calibration in pipe networks. Journal of Hydraulic Research 41 (5), 481–492.

Kim, S. H., 2005. Extensive development of leak detection algorithm by impulse response method. Journal of Hydraulic Engineering 131 (3), 201–208.

Kim, S. H., 2008. Address-Oriented Impedance Matrix Method for Generic Calibration of Heterogeneous Pipe Network Systems. Journal of Hydraulic Engineering, ASCE 134 (1), 66–75.

Kim, S. H., 2015. Impedance Method for Abnormality Detection of a Branched Pipeline System. Water Resources Management 30 (3), 1101–1115.

Lagarias, J. C., Reeds, J. A., Wright, M. H., Wright, P. E., 1998. Convergence properties of the Nelder-Mead simplex method in low dimensions. Siam Journal on Optimization 9 (1), 112–147.

Lee, P. J., Vítkovský, J. P., Lambert, M. F., 2005a. Frequency domain analysis for detecting pipeline leaks. Journal of Hydraulic Engineering 131 (7), 596–604.

Lee, P. J., Vítkovský, J. P., Lambert, M. F., Simpson, A. R., Liggett, J. A., 2005b. Leak location using the pattern of the frequency response diagram in pipelines: a numerical study. Journal of Sound and Vibration 284 (3-5), 1051–1073.

Lee, P. J., Vítkovský, J. P., Lambert, M. F., Simpson, A. R., Liggett, J. A., Murray, S., 2004. Frequency response leak detection using inline valve closure. 9th International Conference on Pressure Surges 1 (239-253).

Liggett, J. A., Chen, L. C., Aug. 1994. Inverse Transient Analysis in Pipe Networks. Journal of Hydraulic Engineering 120 (8), 934–955.

Pezzinga, G., Brunone, B., Meniconi, S., 2016. Relevance of Pipe Period on Kelvin-Voigt Viscoelastic Parameters: 1D and 2D Inverse Transient Analysis. Journal of Hydraulic Engineering 142 (12), 04016063.

Shamloo, H., Haghighi, A., 2010. Optimum leak detection and calibration of pipe networks by inverse transient analysis. Journal of Hydraulic Research 48 (3), 371–376.

Soares, A. K., Covas, D. I. C., Reis, L. F. R., 2011. Leak detection by inverse transient analysis in an experimental PVC pipe system. Journal of Hydroinformatics 13 (2), 153–166.

Stephens, M. L., Lambert, M. F., Simpson, A. R., 2012. Determining the internal wall condition of a water pipeline in the field using an inverse transient. Journal of Hydraulic Engineering 139 (3), 310–324.

Sun, J., Wang, R., Duan, H.-F., 2016. Multiple-fault detection in water pipelines using transient-based time-frequency analysis. Journal of Hydroinformatics 18 (6), 975–989.

Tuck, J., Lee, P., 2013. Inverse transient analysis for classification of wall thickness variations in pipelines. Sensors 13 (12), 17057–17066.

Vitkovsky, J. P., Lambert, M. F., Simpson, A. R., Liggett, J. A., 2007. Experimental observation and analysis of inverse transients for pipeline leak detection. Journal of Water Resources Planning and Management-ASCE 133 (6), 519–530.

Vitkovsky, J. P., Lambert, M. F., Simpson, A. R., Wang, X.-J., et al., 2001. An experimental verification of the inverse transient technique for leak detection. In: 6th Conference on Hydraulics in Civil Engineering: The State of Hydraulics; Proceedings. Institution of Engineers, Australia, p. 373.

Vitkovsky, J. P., Simpson, A. R., Lambert, M. F., 2000. Leak detection and calibration using transients and genetic algorithms. Journal of Water Resources Planning and Management-ASCE 126 (4), 262–265.

Weinerowska-Bords, K., 2006. Viscoelastic model of waterhammer in single pipeline-problems and questions. Archives of Hydro-Engineering and Environmental Mechanics 53 (4), 331–351.

Wylie, E. B., Streeter, V. L., 1993. Fluid transients in systems. Prentice Hall Englewood Cliffs, NJ.

Zecchin, A. C., Lambert, M. F., Simpson, A. R., 2010. Frequency-Domain Modeling of Transients in Pipe Networks with Compound Nodes Using a Laplace-Domain Admittance Matrix. Journal of Hydraulic Engineering, ASCE 136 (10), 739–755.

Zecchin, A. C., Lambert, M. F., Simpson, A. R., White, L. B., Jun. 2014. Parameter Identification in Pipeline Networks: Transient-Based Expectation-Maximization Approach for Systems Containing Unknown Boundary Conditions. Journal of Hydraulic Engineering-ASCE 140 (6), 04014020–12.

Zecchin, A. C., Simpson, A. R., Lambert, M. F., White, L. B., Vitkovsky, J. P., Jun. 2009. Transient Modeling of Arbitrary Pipe Networks by a

Laplace-Domain Admittance Matrix. Journal of Engineering Mechanics-ASCE 135 (6), 538–547.